AAEC/TM344

AAEC/TM344

AUSTRALIAN ATOMIC ENERGY COMMISSION
RESEARCH ESTABLISHMENT
LUCAS HEIGHTS

THERMAL AND STRESS PERFORMANCE OF A PEBBLE BED REACTOR

by

P.A.E. HAWKER

September 1966

AUSTRALIAN ATOMIC ENERGY COMMISSION
RESEARCH ESTABLISHMENT
LUCAS HEIGHTS

THERMAL AND STRESS PERFORMANCE OF A PEBBLE BED REACTOR

by

P.A.E. HAWKER

ABSTRACT

A method for determining the thermal and stress performance of a pebble bed reactor is described.

Some results based on this analysis are presented to indicate the likely trends.

CONTENTS

1. INTRODUCTION

The power density that can be achieved in a pebble bed reactor core is subject to restrictions from material temperature limitations, levitation of pebbles if the coolant normally flows upward, and material strength.

The analysis described in this report is an attempt to synthesize all relevant data to predict the thermal and stress performance of a randomly packed, cylindrical, pebble bed reactor core with plane inlet and outlet faces, subject to these limitations. The analysis has been coded for the IBM 7040 computer (Hawker et al. 1966).

2. METHOD OF SOLUTION

2.1 Core Subdivision and Voidage Distribution

The core is subdivided into a number of annular elements by cylindrical surfaces concentric with the axis of the core, and equispaced planes perpendicular to the axis. An equispaced radial subdivision is made of the region from the axis to a distance four-and-a-half ball diameters from the side wall. The divisions near the wall are four of one pebble diameter spacing and one of half a pebble diameter adjacent to the wall. For isothermal flow, such a subdivision gives results, in terms of the ratio W of mass-velocity on the central axis to the average value, which compare favourably with experimental results.

Within the annular region between the wall and four-and-a-half ball diameters from the wall, the voidage distribution is taken as regular and is made to correspond to published data (Sanderson and Porter 1961; Benenati and Brosilow 1962). Outside this region the voidage for any cell is randomly selected on the basis of a normal distribution about a mean value, chosen as that value to which the regular distribution near the wall tends in its approach towards the central axis. The standard deviation σ_c is taken such that the difference between the mean and 0.2595 (the minimum possible voidage) is $4\ \sigma_c \sqrt{n}$, where n is the number of balls that would be in the cell (Ebeling 1965, Private Communication). Any value chosen outside the range 0.2595 to 1.0 would be rejected. This procedure appears to be justified on the basis of the shape of frequency distributions for the number of points of contact of balls in a randomly packed bed (Wadsworth 1960). In the work described here however, voidage variations away from the walls were found to be insignificant owing to the size of the elemental volumes chosen.

2.2 Temperature Distribution

The method used for determining the gas flow and temperature distribution through the core is similar to that used by Sanderson and Porter (1961) and

gives results in close agreement with those obtained by Pruschek (1962) by a different method. No allowance has been made for the effective radial thermal conductivity of the bed (Yagi and Kunii 1957). For the high Reynolds numbers which occur in the reactor, this is likely to be of minor consequence in relation to the heat transport axially through the pebble bed.

Friction factor data obtained so far on randomly packed beds were determined from overall measurements. It is currently assumed that these data apply locally whatever the size or position of the cell. Sanderson and Porter show that the results of a number of investigators are reasonably correlated on the basis of an assumed dependence of $f' = \frac{\Delta P}{L} \frac{\rho g D_P}{2G^2} \left(\frac{c^3}{1-c}\right)$ on $Re' = GD_P \Big/ \left\{ \mu(1-c) \right\}$.

The method used in this analysis ensures, through iteration, that the mass flow distribution over each plane of subdivision perpendicular to the core axis is such that the value of :

$$\frac{dP}{dz} = \frac{2f'}{gD_P} \left(\frac{1-c}{c^3}\right) \frac{G^2}{\rho} ,$$

for each radial subdivision is the same, the outlet gas temperature for each cell being calculated using the heat generated within the cell and the appropriate values of mean axial mass flow and specific heat.

The surface-to-gas temperature difference is given by:

$$\theta_s - T = \frac{q_b D_P}{6h} ,$$

where h, the heat transfer coefficient, is obtained from Denton et al. (1949), using the correlation based on $\frac{hPr^{0.66}}{G\, c_p}$ and Re'.

For a homogeneous ball, the difference between the temperatures at the ball centre and the surface, for spherically symmetric conditions, is given by:

$$\theta_c - \theta_s = \frac{q_b D_P^2}{24k} ,$$

where k, the conductivity of the pebble material, is taken at a mean value within the ball, determined iteratively.

2.3 Levitation

When the coolant normally flows upward through the reactor core, it appears desirable to ensure that agitation of the pebbles does not occur. Even with isothermal flow this phenomenon is noticed to occur first at the top layer of balls. Therefore, at the top layer:

$$\frac{dP}{dz} \leqslant \xi (1-c) \rho_b .$$

As the voidage is highest near the side wall, the average voidage over one ball diameter from the wall would invariably dictate the limitation on $\frac{dp}{dx}$ at the top. If levitation proves to be a restrictive criterion, the core shape is changed to that of a frustum of a cone of small included angle with the larger face at the top (Hayes and Michel 1965, Private Communication). The code ensures that whilst the limitation at the top is met, the total upward thrust through pressure loss is not greater than the weight of the bed of pebbles:

$$\int \frac{dP}{dz} A\, dz \leqslant \eta \rho_b \int (1-c)\, dv .$$

ξ is a factor to avoid any sign of levitation and to cover dispersion of data for friction factor and levitation. η is a factor to cover dispersion of friction factor data. In the case of the tapered bed, the diameter of the cylinder of equal volume and same length (equivalent diameter) is used in the specification of core shape in terms of length-to-diameter ratio.

2.4 Stress

The high average outlet gas temperatures considered, in conjunction with non-uniform radial distribution of heat generation could result in a region of sufficiently high pebble temperature that, with beryllia based pebbles, creep could be significant.

The following analysis for the thermal stress history of a pebble has been coded separately for the IBM 7040 and will ultimately be included in the main code. The fuel element can consist of a number of concentric regions of which the innermost one could be hollow.

On the basis of spherical symmetry, the heat conduction equation reduces to:

$$\frac{1}{\rho_b s} \left(\frac{1}{r^2} \frac{\partial}{\partial r} \left(r^2 k \frac{\partial \theta}{\partial r} \right) + q_b \right) = \frac{\partial \theta}{\partial t} , \qquad (1)$$

q_b being taken as uniform for the heat generating region, otherwise zero. The pebble is subdivided radially, such that within each region the subdivision is equispaced. To facilitate inclusion of the difference in parameters between regions in boundary conditions, the radius of an interface between two solid regions of the element is counted twice, once as belonging to the inner region and once to the outer region, that is, if i is the index for the first count

of the interface radius, $r_i = r_{i+1}$. Using the following finite difference scheme:

$$\left(\frac{\delta f}{\delta r}\right)_{j+\frac{1}{2}} = \frac{f_{j+1} - f_j}{\delta r} \quad ,$$

$$\left(\frac{\delta f}{\delta r}\right)_{j} = \frac{f_{j+\frac{1}{2}} - f_{j-\frac{1}{2}}}{\delta r} \quad ,$$

where $f_{j+\frac{1}{2}} = \left(f_{j+1} + f_j \right) \Big/ 2,$

Equation 1 can be transformed, giving:

$$\left(\theta_j\right)_{t+\Delta t} = \left(\theta_j\right)_t + \Delta t \frac{1}{\rho_j s_j} \left[\frac{1}{r_j^2}\left\{\frac{(r_{j+1}+r_j)^2(k_{j+1}+k_j)\ (\theta_{j+1}-\theta_j)}{4\,\delta r^2} - \frac{(r_j+r_{j-1})^2(k_j+k_{j-1})\ (\theta_j-\theta_{j-1})}{4\delta r^2}\right\} + q_{b_j}\right],$$

for all j except those corresponding to the innermost and outermost radii of the fuel element and to the interfaces.

To satisfy boundary conditions, three-point Lagrangian differentiation is used (Kopal 1955).

At the innermost radius the boundary condition:

$$\left(\frac{\partial\theta}{\partial r}\right)_{r=r_1} = 0$$

becomes $\theta_1 = \frac{4\theta_2-\theta_3}{3}$.

At interfaces, where i is the index for the first count of the interface radius,

$$\theta_i = \theta_{i+1}$$

and the other boundary condition:

$$\left(k\frac{\partial\theta}{\partial r}\right)_{r=r_i} = \left(k\frac{\partial\theta}{\partial r}\right)_{r=r_{i+1}} \quad ,$$

becomes:

$$\theta_i = \left\{\left(4\theta_{i+2}-\theta_{i+3}\right) k_{i+1} \Big/ \delta r_{m+1} + \left(4\theta_{i-1} - \theta_{i-2}\right) k_i \Big/ \delta r_m\right\} \Big/ \left\{3\left(k_i \Big/ \delta r_m + k_{i+1} \Big/ \delta r_{m+1}\right)\right\},$$

where m is the index used for the count of regions.

At the outermost radius r_n, the boundary condition is:

$$-\left(k\frac{\partial\theta}{\partial r}\right)_{r=r_n} = h\left(\theta_n - T\right),$$

where h is the heat transfer coefficient, convective in the core (Section 2.2), with T as gas temperature. However, if it is assumed that immediately after sintering (the last manufacturing operation) the element cools down only by radiation to a large enclosure at temperature T, then

$$h = \zeta\ e\left(\theta_n + T\right)\left(\theta_n^2 + T^2\right).$$

Kelly (1964) indicates that the creep rate $\dot{\epsilon}$ in beryllia under uni-axial tension obeys a law of the form:

$$\dot{\epsilon} = A\,\sigma \exp\left(-\frac{D}{\theta}\right) .$$

Following Shorr (1962), using the concept of the strain rate intensity:

$$\dot{\epsilon}_i = A\,\sigma_i \exp\left(-\frac{D}{\theta}\right) ,$$

where $\dot{\epsilon}_i = \frac{2}{3}\left|\dot{\epsilon}_r - \dot{\epsilon}_t\right|,$

we get $\dot{\epsilon}_{pr} = A \exp\left(-\frac{D}{\theta}\right)\left(\sigma_r - \sigma_t\right),$

and $\dot{\epsilon}_{pt} = \frac{1}{2}\ A \exp\left(-\frac{D}{\theta}\right)\left(\nu\,\sigma_r - \sigma_t\right)$

The total creep strain at any point is calculated from:

$$\left(\epsilon_{pr,t}\right)_{t+\Delta t} = \left(\epsilon_{pr,t}\right)_t + \left(\dot{\epsilon}_{pr,t}\right)_t \Delta t .$$

Smith (1965) has given in detail a method for determining the variation with time of the stress field in solid and hollow spheres. A simple combination of his Tables 4 and 5, with obvious modifications to account for the different boundary conditions, is used in this analysis. The boundary condition at the innermost radius is:

$$\sigma_{r_1} = 0 \qquad \text{if } r_1 > 0 \ ,$$

or

$$\sigma_{r_1} - \sigma_{t_1} = 0 \qquad \text{if } r_1 = 0.$$

The boundary conditions at interfaces are:

$$\sigma_{r_i} - \sigma_{r_{i+1}} = 0 \ ,$$

and

$$\frac{1}{E_i}\left[\sigma_{t_i}(1-\nu_i) - \nu_i \sigma_{r_i}\right] + \epsilon_{pt_i} + \alpha_i \theta_i =$$

$$\frac{1}{E_{i+1}}\left[\sigma_{t_{i+1}}(1-\nu_{i+1}) - \nu_{i+1}\sigma_{r_{i+1}}\right] + \epsilon_{pt_{i+1}} + \alpha_{i+1}\theta_{i+1} \ ,$$

where $r_i = r_{i+1}$.

The boundary condition at the outermost radius is:

$$\sigma_{r_n} = 0.$$

Each time interval Δt is evaluated from

$$(\Delta t) = (\ell n R) \Big/ \left\{ - AE_n \exp(-D/\theta_n) \right\} \ ,$$

where R is a fraction found by trial, so the time interval corresponds to the rate of relaxation. If, within the core, addition of this time interval would take the pebble past the next horizontal subdivisional plane, the time interval to arrive at this plane is taken instead.

Currently, the code TASPOP only evaluates the thermoelastic stress at each mesh point of the reactor core in terms of a thermal stress parameter for a homogeneous ball:

$$\sigma^* = \frac{\sigma_{t_n}}{\frac{E_n \alpha_n}{1-\nu_n}\frac{1}{k_n}} = \frac{q_b D_P^2}{60} \ ,$$

the maximum tensile stress occurring at the surface of a pebble.

A fuel management scheme was chosen for analysis in which the fuel is passed several times through the core. It is assumed that the method of feeding pebbles at the top of the core is such that any pebble has an equal probability of starting its motion at any radial position. It is also assumed that a pebble remains at the same radius on its way through the bed and that all pebbles move at a constant velocity. Thus the fraction of balls in a cell that are passing through the core for the n^{th} time is assumed equal to that for any other pass,

though the failure rate for the passes would differ.

As the properties of ceramics are not clearly defined, the performance is gauged in terms of probability of failure, using the thermal stress parameter as the basis. This procedure is assumed to hold even when creep and irradiation growth are included.

If, corresponding to the conditions at any point in the life of a pebble, the thermal stress parameter is characterized by a mean value σ_m^* and a standard deviation σ, and the maximum demand value for the pebble is σ_d^*, the probability of failure is given by the cumulative normal distribution function:

$$\frac{1}{2} + \frac{1}{\sqrt{2\pi}\,\sigma} \int_{\sigma_m^*}^{\sigma_d^*} e^{-(t-\sigma_m^*)^2/(2\sigma^2)} \, dt \ ,$$

which for computational convenience is transformed to:

$$\frac{1}{2}\left\{1 + \operatorname{erf}\left(\frac{\sigma_d^* - \sigma_m^*}{\sqrt{2}\,\sigma}\right)\right\} \ . \qquad \text{.....(2)}$$

On each pass, the value obtained for the failure fraction at a particular radius on a horizontal subdivisional plane is multiplied by the number of balls of that pass and same history in the cell corresponding to that radius and immediately below that plane, to give the probable number of failed balls within that cell. Summing this quantity over the whole core gives the total number failed within the core for that pass and history.

If on a particular pass the probability of failure at a mesh point, based on the demand value of thermal stress parameter at that point, is less than a previous value on that pass (that is, at any mesh point vertically above), the latter is taken as the failure fraction. On the second and subsequent passes, the highest probability of failure value of the previous pass or passes must be subtracted from current values of (2) to give the probability of failure, only successful balls being recirculated. Of course, if this difference is negative the probability of failure is zero.

Considering the second pass and referring to an annulus of the core subdivision as a column, it is assumed that the fraction of second pass balls in a cell that have passed through a certain column on the first pass is equal to the ratio of the volume of that column to the volume of the whole bed. So far, only the first and second passes have been incorporated in the code TASPOP, and the results indicate that calculating the total number of failed balls from these

two passes only could be adequate, because even the second pass contributes only a small fraction of the total.

In the case of upflow of coolant, as an interim measure creep is now approximately taken into account by assuming that complete relaxation of stress takes place at temperatures above 900°C with no relaxation at all below this temperature, and that any pebble failures occur only in that annulus of the core in which pebbles have not been affected by creep.

2.5 General

Although a statistical probability of failure criterion is applied to the thermal stress resistance of the fuel element material, a simple product-of-factors method is used for all other uncertainties in estimation of the thermal stress in a pebble since many of the uncertainty factors are inadequately known. The factors included cover pebble coating, transients, non-uniform heat transfer coefficient around a pebble, and dispersions in data, fuel concentration, and dimensions.

Iteration, covering the computation corresponding to the analysis described in Sections 2.1 to 2.4, involving changes in core size if stress limited, or ball diameter if levitation limited in the case of upflow, proceeds until the change in total pressure drop across the core is not significant. Total thermal output, coolant inlet pressure and temperature, coolant average outlet gas temperature, and core length-to-equivalent-diameter ratio are maintained constant at the initially selected values.

3. RESULTS AND DISCUSSION

Computed values of the ratio, W, of gas mass-velocity on the central axis to the average value, as a function of the bed-to-ball diameter ratio D/Dp, are compared with those of experimental data for isothermal flow (Schwartz and Smith 1953; Collins 1958; Dorweiller and Fahien 1959; Bundy 1964), in Figure 1.

The remaining results are based on the properties of unirradiated BeO, and CO_2, and the following values:

Total thermal output of core	500 MW
Inlet pressure of CO_2	40 atmospheres
Length-to-diameter ratio of core	0.6
Inlet gas temperature	300°C
Average outlet gas temperature	800°C
Factor on stress parameter	1.64

Factor on gas temperature rise	1.1
Factor on surface-to-gas temperature difference	1.32

$\xi = 0.85$

$\eta = 0.9$

The correlations for heat transfer and friction factor obtained by Denton et al. (1949) were used. Average core power density distributions were taken as cosine. Distributions over the core volume of the ratios of ball power density, first pass to average, and second pass to average, were deduced from results supplied by Bicevskis (1965, Private Communication).

The average core power density q obtainable in each case is expressed as a ratio relative to the downflow case with uniform average power density q_o, ball diameter 3.81 cm, allowable failure fraction 0.001, $\sigma/\sigma_m^* = 0.1555$, and without creep and irradiation growth.

Figures 2 to 5 show, for downflow, the variations of q/q_o with radial form factor f_r, pebble diameter D_p, allowable failure fraction FF, and ratio of standard deviation to mean value of thermal stress parameter SIG = $\frac{\sigma}{\sigma_m^*}$, ignoring the effects of creep and irradiation growth, and keeping the axial form factor f_a constant. The variations of mass-velocity ratio, W, and maximum gas and pebble temperatures, with radial form factor are indicated in Figures 6 and 7.

When the coolant flows upward with $f_a = 1.3$, $f_r = 1.4$, $D_p = 3.81$ cm, FF = 0.001, and SIG = 0.1555, ignoring creep and irradiation growth, a value of 0.487 is obtained for q/q_o. Allowing approximately for creep, as indicated in Section 2.4, and using FF = 0.001 as applicable to failures within the core only, the value for q/q_o is 0.7. The variation with radial form factor is presented in Figure 8. However, these must be optimistic estimates as the residual stresses in pebbles affected by creep would result in some failure rate on exit from the core. Preliminary estimates indicate this failure rate to be rather higher than that within the core. The total failure rate, considering the whole life of a pebble, can be computed if the separate programme for thermal stress history of a pebble, described in Section 2.4, and irradiation growth, are incorporated in the main code, TASPOP.

It is interesting to note that, for the same ball diameter, though the other parameters vary over wide ranges, the power density q_o for the reference case is invariably greater, owing mainly to the uniform radial power density distribution, and to a lesser extent to the more favourable axial power density distribution relative to the mean thermal stress parameter variation in a downflow

reactor core.

In all the cases considered, the failure criterion happened to be the operative restriction. For upflow, based solely on the levitation criteria whilst suppressing the stress limitation, Figure 9 shows for a fixed ball diameter, the obtainable average core power density variation with radial form factor. Comparison with Figure 8 indicates the margin between the two limitations. This may be reduced by decreasing the coolant pressure at the expense of pressure loss through the core which for the cases of Figure 8 is about 4.5 p.s.i.

4. ACKNOWLEDGEMENT

The author is indebted to Mr. N.W. Ridgway for his assistance with computation and presentation of the results.

5. REFERENCES

Benenati, R.F., and Brosilow, C.B. (1962). - Void fraction distribution in beds of spheres. Am. Inst. Chem. Engrs. J. 8 : 359.

Bundy, R.D. (1964). - An experimental study of random beds of spheres packed in a vessel having non-uniform end geometry. Second Southeastern Conference on Theoretical and Applied Mechanics, April 1964, Atlanta, Georgia.

Collins, M. (1958). - Velocity distribution in packed beds. Master's Thesis, University of Delaware, Newark, Delaware.

Denton, W.H., Robinson, C.H., and Tibbs, R.S. (1949). - The heat transfer and pressure loss in fluid flow through randomly packed spheres. AERE, H.P.C. 35.

Dorweiller, V.P., and Fahien, R.W. (1959). - Mass transfer at low flow rates in a packed column. Am. Inst. Chem. Engrs. J. 5 (2) : 139.

Hawker, P.A.E., Plotnikoff, W.W., and Ridgway, N.W. (1966). - TASPOP - Thermal and stress performance of a pebble bed reactor. A.A.E.C. Report in preparation.

Kelly, J.W. (1964). - The creep of beryllium oxide - A literature survey. AAEC/TM274.

Kopal, Z. (1955). - Numerical Analysis. Chapman and Hall, London.

Pruschek, Von R. (1962). - Temperature distribution and coolant flow through a gas cooled reactor. Atomkernenergie 8 : 161.

Sanderson and Porter, New York (1960). - Progress Report - Pebble bed reactor program, Period of June 1959 - Oct. 1960, NYO-9071.

Schwartz, C.E., and Smith, J.M. (1953). - Flow distribution in packed beds. Ind. and Engng. Chem. 45 (6) : 1209.

Shorr, B.F. (1960). - Fundamentals of creep calculations on non-uniformly heated parts. Strength and Deformation in Non-uniform Temperature Fields, ed. by Ya. B. Fridman. Consultants Bureau, N.Y. p116.

Smith, E.M. (1965). - Analysis of creep in cylinders, spheres and thin discs. J. Mech. Engng. Sci. 7 (1) : 82.

Wadsworth, J. (1960). - Experimental examination of local processes in packed beds of homogeneous spheres. NRC Report MT-41.

Yagi, S. and Kunii, D. (1957). - Studies on effective thermal conductivities in packed beds. Am. Inst. Chem. Engrs. J. 3 (3) : 373.

APPENDIX 1

NOTATION

A	cross-sectional area of core and a creep rate constant
c	voidage
c_P	specific heat of gas
D	bed diameter and a creep rate constant
D_P	pebble diameter
e	emissivity of ball surface
f	arbitrary function
f_a	axial form factor
f_r	radial form factor
f'	modified friction factor
FF	allowable failure fraction within core
g	gravitational constant
G	mass-velocity of gas (= ρv)
h	heat transfer coefficient
j	index for count of radial subdivision in pebble
k	thermal conductivity of ball material
L	length of core
n	total number of subdivisional points on radius of ball
P	pressure of gas
Pr	Prandtl number
q	core average power density
q_b	ball power density
q_o	core average power density for downflow core reference case
r	radial coordinate in ball
R	fraction for time step
Re'	modified Reynolds number
s	specific heat of pebble material
SIG	$= \frac{\sigma}{\sigma^*_m}$
t	time
T	temperature of gas or enclosure for radiation
v	volume of core
W	mass-velocity ratio
z	axial coordinate in core
α	thermal linear coefficient of expansion of ball material
ϵ_i	strain intensity (Shorr)
$\epsilon_{pr,t}$	radial and tangential creep strain components
μ	viscosity of gas
ν	Poisson's ratio for ball material
ρ	density of gas
ρ_b	density of pebble material
σ	standard deviation of thermal stress
$\sigma_{r,t}$	radial and tangential stress components
σ_c	standard deviation for voidage
σ_i	stress intensity (Shorr)
σ^*	thermal stress parameter
σ^*_d	demand value of thermal stress parameter
σ^*_m	mean value of " " "
θ	ball temperature
θ_c	ball centre temperature
θ_s	ball surface temperature
ξ	factor for levitation
η	" " "
ζ	Boltzmann's constant
ΔP	pressure loss across core
Δt	time interval

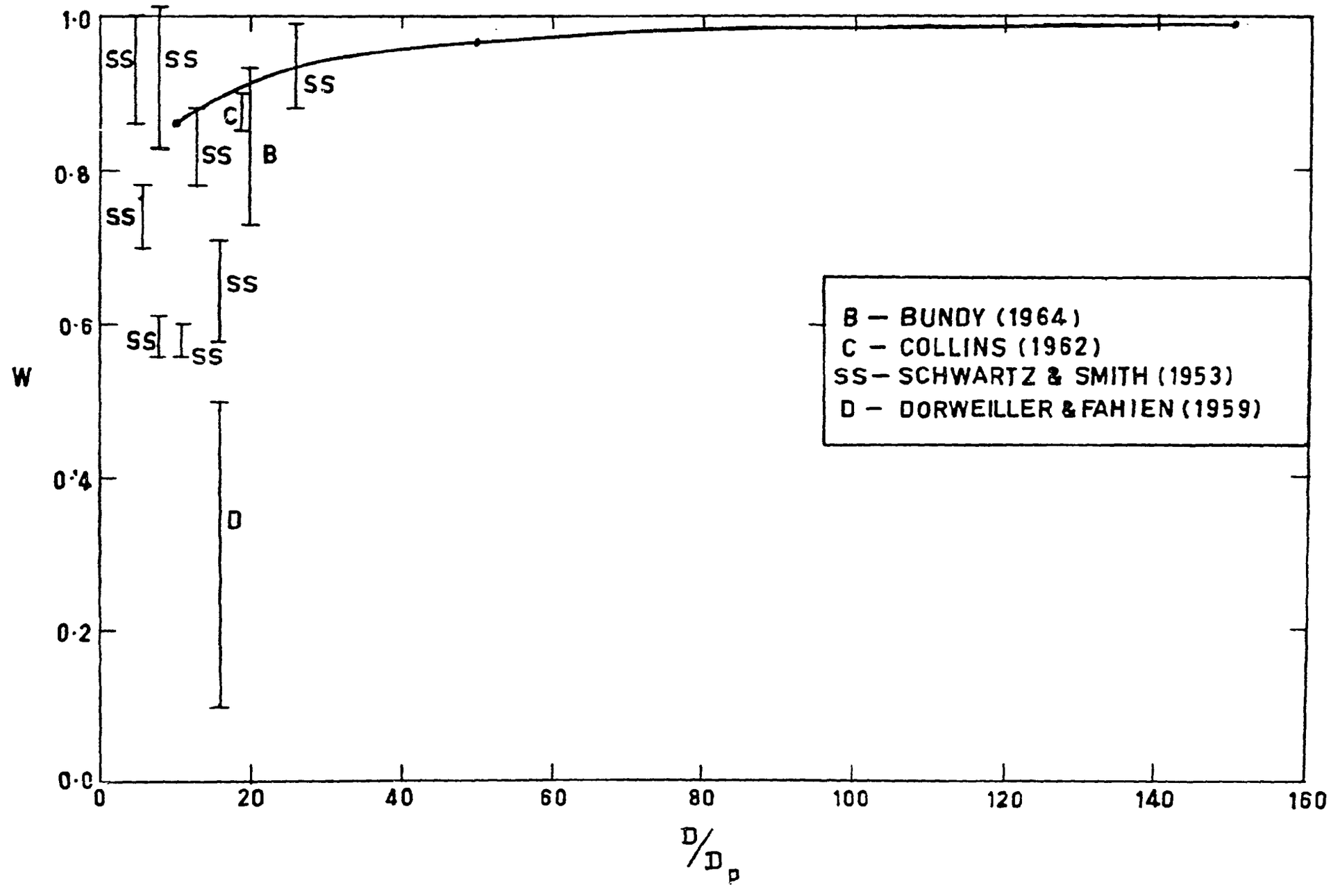

FIGURE 1. MASS FLOW RATIO v. BALL/BED DIAMETER RATIO (ISOTHERMAL CASE)

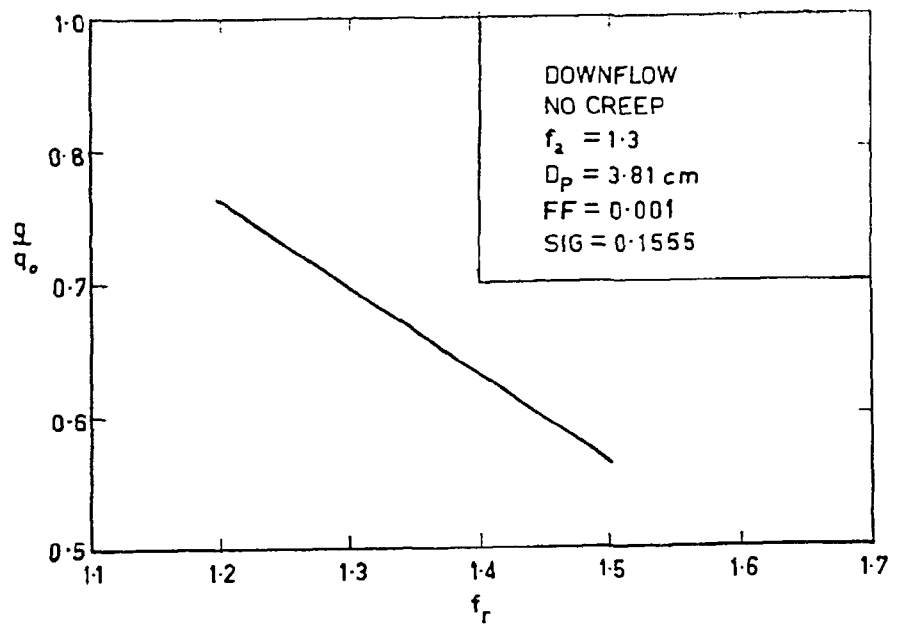

FIGURE 2. POWER DENSITY RATIO v. RADIAL FORM FACTOR

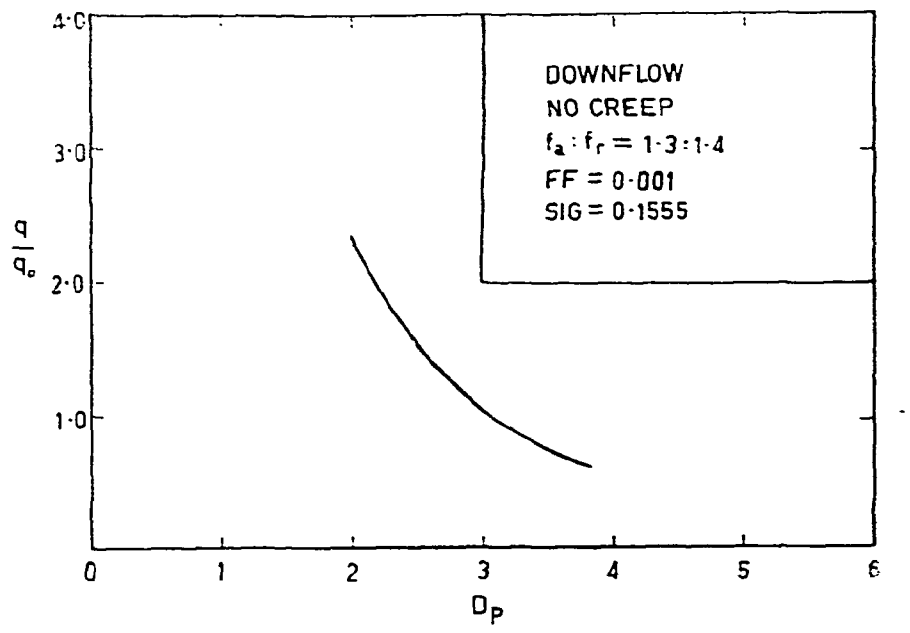

FIGURE 3. POWER DENSITY RATIO v. BALL DIAMETER

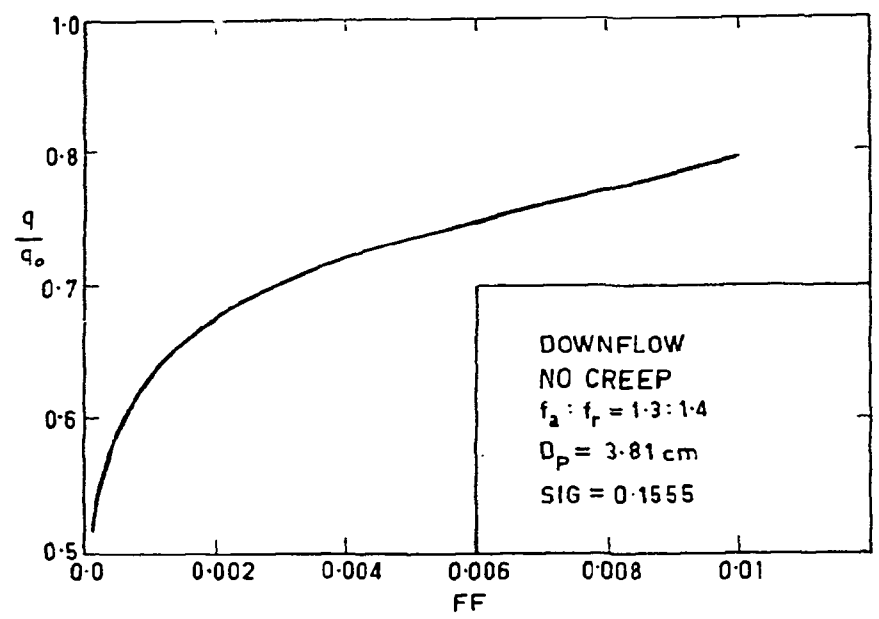

FIGURE 4. POWER DENSITY RATIO v. BALL FAILURE FRACTION

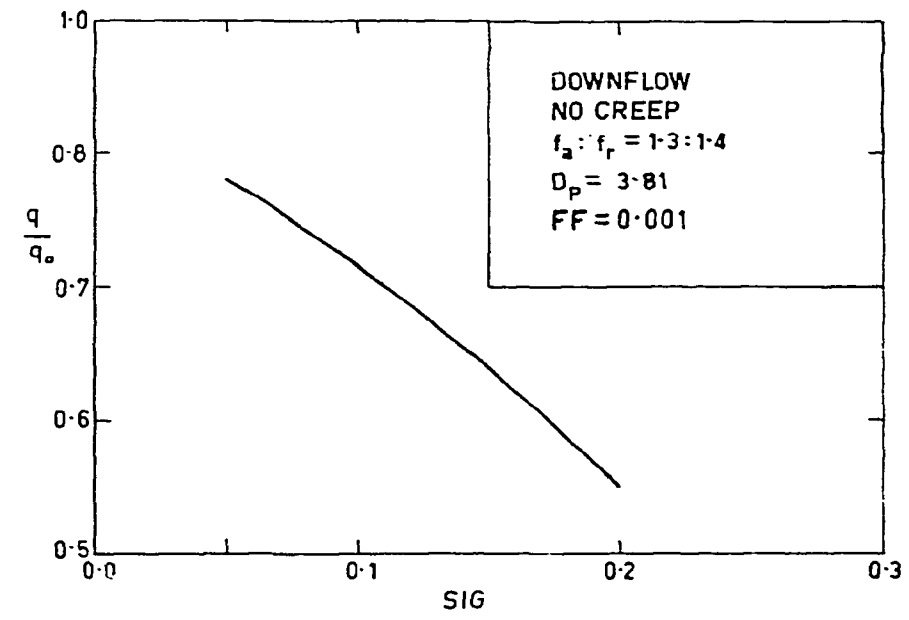

FIGURE 5. POWER DENSITY RATIO v. STANDARD DEVIATION RATIO

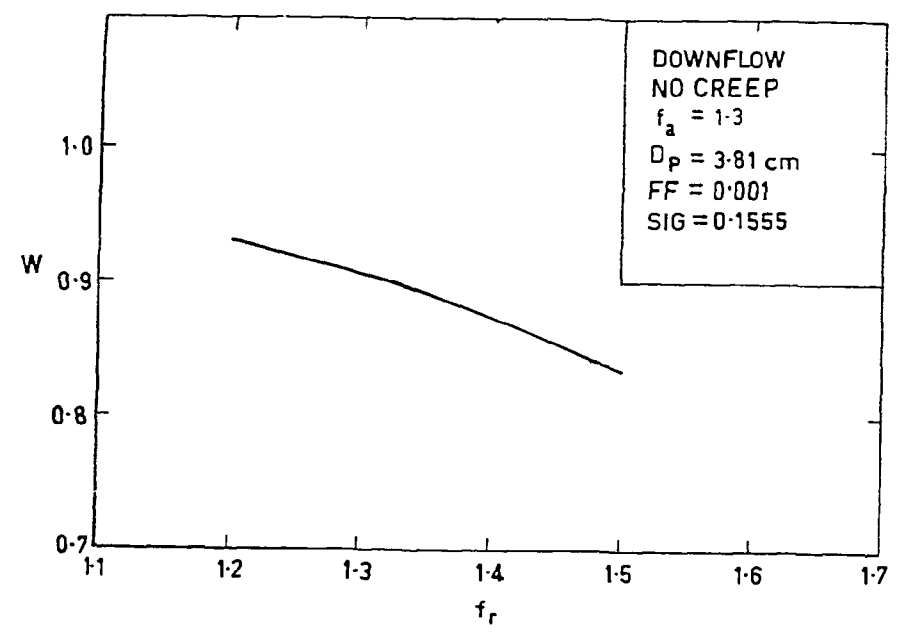

FIGURE 6. MASS FLOW RATIO v. RADIAL FORM FACTOR

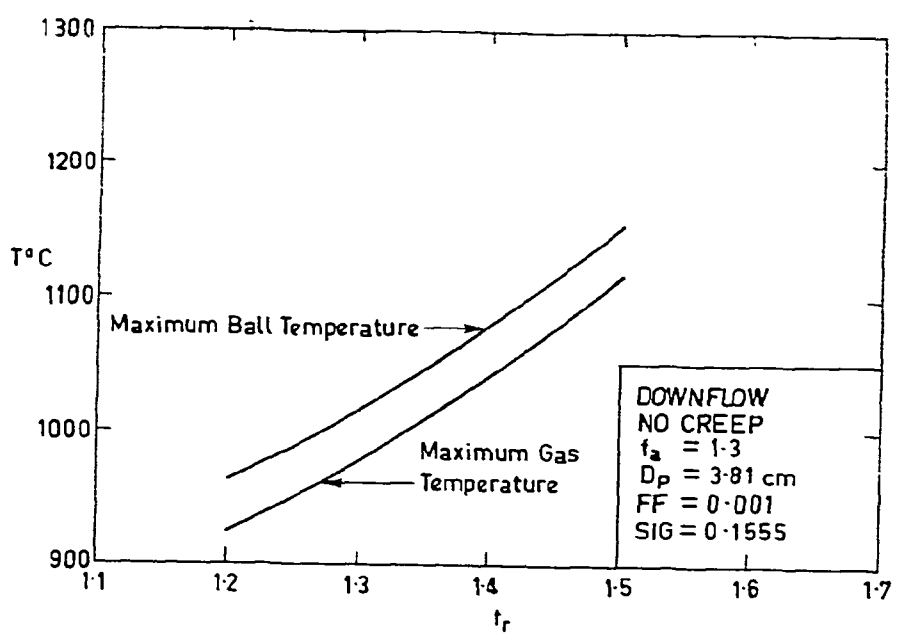

FIGURE 7. TEMPERATURE v. RADIAL FORM FACTOR

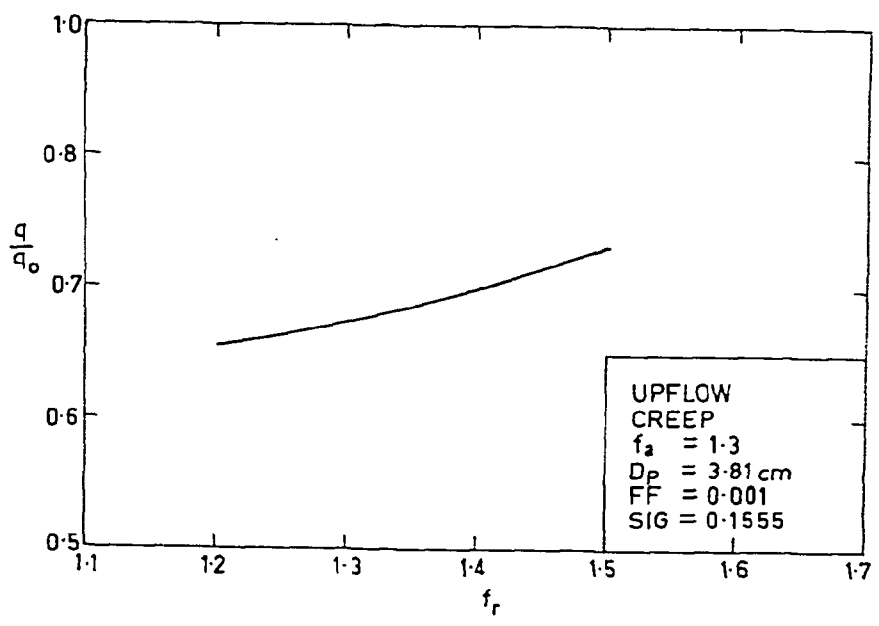

FIGURE 8. POWER DENSITY RATIO v. RADIAL FORM FACTOR

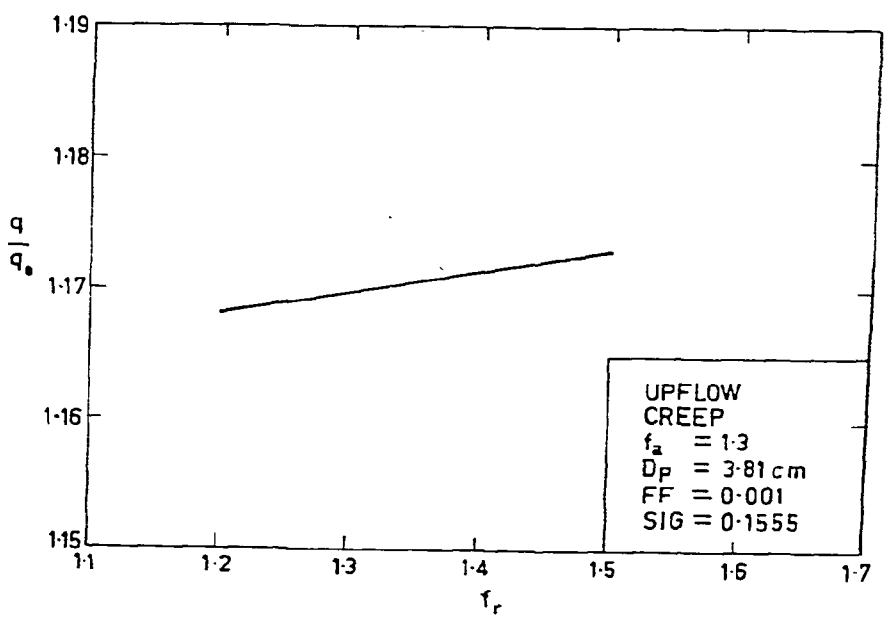

FIGURE 9. POWER DENSITY RATIO v RADIAL FORM FACTOR (LEVITATION LIMITED, STRESS LIMITATION SUPPRESSED)